Effect of Gas Diffusion on Mobility of Foam for Enhanced Oil Recovery

Nonnekes, Lars E.; Cox, Simon J.; Rossen, William R.

Published in:
Transport in Porous Media

DOI:
10.1007/s11242-014-0419-z

Publication date:
2015

Citation for published version (APA):
Nonnekes, L. E., Cox, S. J., & Rossen, W. R. (2015). Effect of Gas Diffusion on Mobility of Foam for Enhanced Oil Recovery. *Transport in Porous Media*, *106*(3), 669-689. https://doi.org/10.1007/s11242-014-0419-z

Effect of Gas Diffusion on Mobility of Foam for Enhanced Oil Recovery

Lars E. Nonnekes[1] · Simon J. Cox[2] · William R. Rossen[1]

1 - Department of Geoscience and Engineering, Delft University of Technology, 2628 CN , Delft, The Netherlands
2 - Institute of Mathematics and Physics, Aberystwyth University

William Richard Rossen
Email: W.R.Rossen@tudelft.nl

Abstract Transport of gas across liquid films between bubbles is thought to increase bubble size in foam in porous media. It is cited as one reason why CO_2 foams for enhanced oil recovery (EOR) are less resistant to flow than N_2 foams and why steam foams are less resistant than foams of steam mixed with N_2. In porous media, diffusion can rapidly destroy bubbles smaller than a pore, but in EOR foam bubbles are thought to be larger than pores.

We examine here the effect of inter-bubble gas diffusion on flowing bubbles in a periodically constricted tube and in particular its effect on the bubble-size distribution and capillary resistance to flow. We use the solution for bubble shapes, curvatures and pressure differences between bubbles from previous studies of bubble movement through periodically constricted tubes to estimate the diffusion rate between bubbles. Bubbles somewhat smaller than a pore can indeed disappear by diffusion as the bubbles move. For bubbles larger than a pore, as expected in EOR, diffusion does not affect bubble size. Instead, diffusion actually increases capillary resistance to flow, because lamellae spend more time in positions where lamella curvature resists forward movement.

When fit to pressures and diffusion and convection rates representative of field application of foams, diffusion is not expected to alter the bubble-size distribution in a foam, but instead modestly increases the resistance to flow. The reason for the apparent weakness of CO_2 foam therefore evidently lies in factors other than CO_2's large diffusion rate through foam.

Keywords Foam ·Diffusion · Enhanced oil recovery · Foam stability ·CO2 foam · Steam foam

1 Introduction

Foam can improve the sweep efficiency of gas injected into oil reservoirs for enhanced oil recovery (EOR) by reducing gas mobility in the formation. Foam in porous media is defined (Hirasaki 1989) as a dispersion of gas in liquid such that the liquid phase is interconnected and at least some of the gas flow paths are blocked by liquid films, called lamellae. In principle "continuous-gas foams" are those where gas flows as a continuous phase around occasional pore throats blocked by lamellae (Falls et al. 1988a). However, most current modeling is based on a picture of a "discontinuous-gas foam," in which gas is separated into discrete bubbles in the porous medium (Falls et al. 1988a; Alvarez et al. 2001; Chen et al. 2010; Afsharpoor et al. 2010; Ashoori et al. 2012). Some fraction of these bubbles is trapped in place, and others move in "bubble trains" through the pore space (Falls et al. 1989). The success of these models in representing foam properties suggests that discontinuous-gas foam is the correct picture of foam in geological formations. These models account for two steady-state flow regimes, a minimum pressure gradient for foam generation, and shear-thinning rheology and nearly fixed bubble size in the "low-quality" regime. It is not clear how a model of continuous-gas foam could account for these phenomena.

The mobility of gas in foam depends on the size of the bubbles (Falls et al. 1989): the larger the bubbles, the more mobile the gas. The bubble size in turn depends on multiple dynamic processes of creating and destroying lamellae in the pore space (Falls et al. 1988a).

For the purposes of this paper on gas diffusion, the gases that are injected for EOR can be classed in three groups, based on their solubility in water and transport rate through lamellae: steam, CO_2 (especially supercritical CO_2), and relatively insoluble gases such as N_2 and CH_4. CO_2 foams are currently of particular interest for EOR because of the ability of CO_2 to miscibly displace oil and the need to reduce greenhouse gases by disposing of industrial CO_2 emissions underground (Enick et al. 2012).

A number of laboratory studies find that CO_2 foams have greater mobility that N_2 foams - in the terminology of foam EOR, the CO_2 foams are "weaker" (Kuhlman 1990; Chou 1991; Kibodeaux 1997; Farajzadeh et al. 2009). A direct, conclusive comparison is difficult, because a surfactant optimized for one gas may not be optimal for another. If CO_2 foams are inherently weaker, then this could mean that the bubbles are larger, though part of the difference could reflect smaller surface tension of CO_2 against surfactant solution (Rossen 1996; Chabert et al. 2012), and the consequent reduced capillary resistance to flow.

There are numerous differences between CO_2 and N_2 foams: greater solubility of CO_2 in surfactant solution; faster diffusion of CO_2 through lamellae (Farajzadeh et al. 2009); lower pH with CO_2 foam; lower surface tension of supercritical CO_2 against the lamella (Rossen, 1996; Chabert et al. 2012); different ionic strength because of dissolved HCO_3 in the aqueous phase of CO_2 foam; greater density and viscosity of the nonaqueous phase with supercritical CO_2; different stability because of different Hamaker constant across the lamella (Kibodeaux 1997), etc. In particular, the faster diffusion of CO_2 through lamellae is cited as a possible cause of this difference between CO_2 and N_2 foam (Farajzadeh et al. 2009).

In bulk (in a container much larger than the bubbles), inter-bubble gas diffusion causes a foam to coarsen: smaller bubbles disappear over time, losing their gas to surrounding larger bubbles until eventually only one bubble is left in the container (Weaire and Hutzler 1999). Rossen (1996), using a schematic picture of stagnant foam in porous media, contends that this process should stop when bubble size is of the same order as the pore size. When all lamellae occupy pore throats, there is no curvature across the lamella to drive further diffusion, whatever the relative volumes of adjacent bubbles. In other words, diffusion rapidly destroys bubbles smaller than pores but has no effect on bubbles larger than pores. Since it is thought that in geological formations foam bubbles are larger than pores (Rossen 1996; Alvarez et al. 2001), diffusion would have little effect on the bubble-size distribution. Cohen et al. (1996) show in a 2D network model with small bubbles initially placed in pore throats that diffusion shrinks the smaller bubbles until they disappear, leaving a foam with one bubble per pore.

Falls et al. (1988b) demonstrate experimentally that adding a small amount of N_2 to a steam foam markedly reduces the mobility of the foam in porous media. They contend that the N_2 reduces the transport of steam through the lamella, and thereby reduces the rate at which small bubbles disappear by transport of steam into adjacent bubbles. For steam, transport across the lamella depends on condensation of steam on one surface and evaporation on the other, with the rate controlled by heat conduction across the lamella. Because the lamella is so thin (10-100 nm) (Kralshevsky et al. 1996) and heat conduction so fast (Bird et al. 2002), transport is rapid. Even a small amount of N_2 slows this down: as water condenses on one side of the lamella, a film rich in N_2 is created in the gas adjacent to the lamella. Water vapor must diffuse through this film to reach the lamella. This diffusion process is much slower than condensation and heat conduction, and the rate of transport is greatly reduced.

Besides diffusion causing the bubble-size distribution to coarsen, there are at least two other possible mechanisms that could link the condensation of steam on lamellae to lamella stability. Marsden (1986) notes that the heat of condensation of water increases with pressure: thus the heat liberated when steam condenses on one side of the lamella is greater than that absorbed by evaporation on the other side. Therefore as the process proceeds, the lamella would heat up and become less stable as temperature increases. In an extreme case the water in the lamella could evaporate. Hatziavrimidis (1992) shows that the process of evaporation from a lamella is inherently unstable because of Marangoni flows: the lamella would thin and break. Thus the findings of Falls et al. (1988b) may reflect rupture of the lamellae in steam foam, not growth of large bubbles by transport of water through the lamellae.

This study examines the effect of gas diffusion on a foam's bubble-size distribution as foam flows through a simplified representation of a bubble train in a porous medium - a periodically constricted tube. We find that for bubbles smaller than a pore, diffusion does increase the average bubble size. In this process a key step is the stranding and bypassing of bubbles in the pore body as lamellae jump across the body. For a foam with bubbles larger than pores, diffusion has no effect on the bubble-size distribution. In that case, diffusion *increases* the capillary resistance to flow: foam appears stronger, not weaker, because of diffusion. For conditions representative of field application, however, we predict the effect of diffusion to be small.

In this paper we focus on results and implications of a 3D model of the bubble train. In 2D (Nonnekes et al. 2012) the results are similar but entail additional complications.

2 Model Description

2.1 Pore Geometry and Lamella Movement

Our model of the porous medium is a periodically constricted tube comprising identical bi-conical pores. Rossen (1990a-d) and Cox et al. (2004) describe the quasi-static movement of lamellae through 2D and 3D periodically constricted tubes. As in those studies, we assume quasi-static movement, so that lamellae are always perpendicular to the pore wall, a geometric constraint that is approximately correct for moving lamellae (Xu and Rossen 2003).

As shown by Rossen (1990a-d) and Cox et al. (2004), a minimum pressure gradient is required to overcome the capillary resistance to foam flow and keep these trains moving; this pressure gradient depends on pore shape, foam texture (i.e., bubble size), and surface tension. It is estimated that about half the mobility reduction in foam arises from the capillary resistance to foam flow (Falls et al. 1989). The shape of the pores mainly determines the shape and curvature of the lamellae, since lamellae must be perpendicular to the pore walls. In 3D these shapes can be complex when they make jumps in the middle of the pores and take on asymmetric shapes. Values for film permeability to gas at low pressure are given by Farajzadeh et al. (2011). These values are used here to estimate realistic choices for parameters describing the driving forces in our model.

The parameters defining pore shape are illustrated in Figure 1. In all results shown here, R_t = 10 μm, R_b = 50 μm, ε=0.05 and L = 100 μm. The sharp corner in the pore body is rounded-off over a distance $\pm(2\varepsilon L)$ = 10 μm around the pore body; this could reflect the effect of capillary pressure (i.e., water filling the pore corner) (Rossen 1988). The lamella jumps over this part of the pore wall (Rossen 1988; Cox et al. 2004).

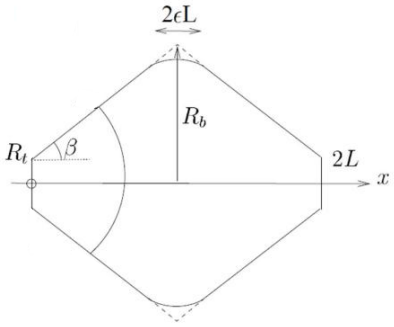

Fig. 1 Parameters defining the geometry of an axisymmetric pore; from Cox et al. (2004)

The lamella moves forward through the pore in five intervals, illustrated schematically in Figure 2 (see also Cox et al. 2004). For each interval the calculations of Cox et al. provide the volume of gas behind the lamella, the area of the lamella, and the mean curvature of the lamella. Briefly, in the first interval the lamella bulges forward in the pore throat. In the second it moves downstream until it reaches the beginning of the rounded pore wall near the pore body. The lamella then jumps at constant volume of gas to a position where it straddles the pore body. In the third interval it moves downstream until it again reaches the rounded pore wall near the pore body, and jumps to a shape attached to the converging pore wall. It then continues toward the pore throat with shapes that are the mirror image of those it had near the upstream pore throat, and finally (Interval 5) flattens in the pore throat, before entering the next pore.

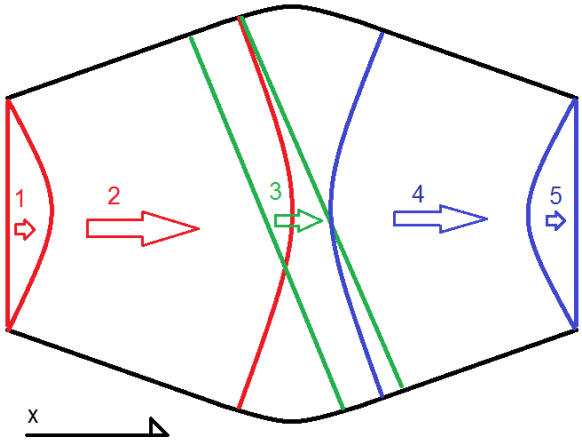

Fig. 2 Schematic of lamella movement through pore. Numbers refer to intervals explained in text. For simplicity, the lamellae in Interval 3 are shown as flat; in reality they are saddle-shaped. The pore throat shown here is wider than that used in calculations

We dimensionalize pressure difference across the lamella by the capillary entry pressure of the pore:

$$\Delta P_D \equiv \frac{4\gamma / R_l}{2\gamma / R_t} = \frac{2R_t}{R_l} \tag{1}$$

where R_l is the radius of the lamella. We dimensionalize volume behind the lamella V by the volume of a pore V_{tot}:

$$V_D \equiv \frac{V}{V_{tot}} \tag{2}$$

while lamella area A is made dimensionless as follows:

$$A_D \equiv \frac{A}{L^2} \tag{3}$$

Figure 3 shows dimensionless pressure difference across the lamella ΔP_D, dimensionless lamella area A_D, and the maximum (x_1) and minimum (x_2) positions of contact along the curved contact between the lamella and the pore wall as the lamella advances across the pore.

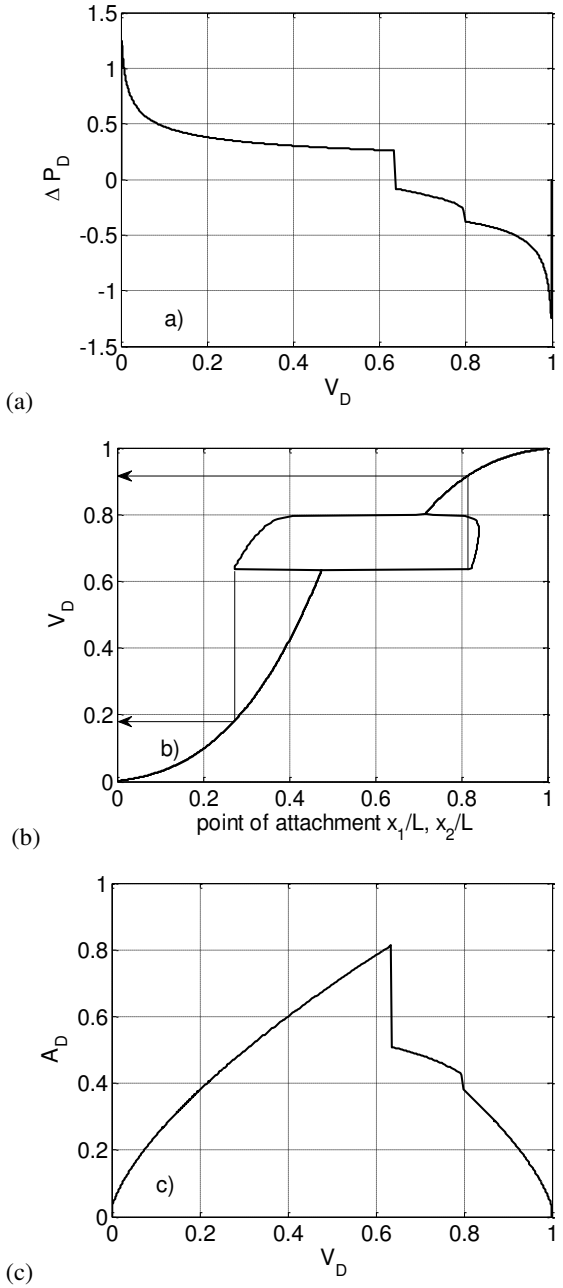

Fig. 3 a) Dimensionless pressure difference across the lamella ΔP_D v dimensionless volume behind the lamellae V_D. The average value of ΔP_D is 0.1067; the standard deviation, 0.3994. **b)** Maximum and minimum positions of contact between the lamella and the pore wall. Arrows illustrate that after first jump the lamella would contact following lamellae with $V_D \geq 0.182$ and lamellae ahead with $V_D \leq 0.919$. **c)** Dimensionless lamella area A_D

Important to what follows are the following aspects of this movement: In Intervals 2 and 4, lamella area is inversely proportional to the square of lamella radius (Figure 3c) while pressure difference across the lamella (Figure 3a) is proportional to the reciprocal of lamella radius. Throughout Interval 3, lamella mean curvature (and therefore pressure difference across the lamellae) is negative. In Intervals 1 and 2, there is a positive pressure difference across the lamella; in Interval 3 it is negative (greater pressure in the forward bubble than the rearward bubble), and increasingly negative as the lamella advances (Figure 3a); and in Intervals 4 and 5 the pressure difference is also negative. At the jump between Intervals 2 and 3, and between Intervals 3 and 4, one side of the lamella moves backwards (Figure 3b). If there were another lamella just ahead or just behind it the two lamella would join and isolate one bubble against the pore body, as shown schematically in Figure 4. For instance, a lamella making the jump from Interval 2 to 3 (at $V_D = 0.637$) would overlap with any lamella with $V_D \geq 0.182$ or $V_D \leq 0.919$.

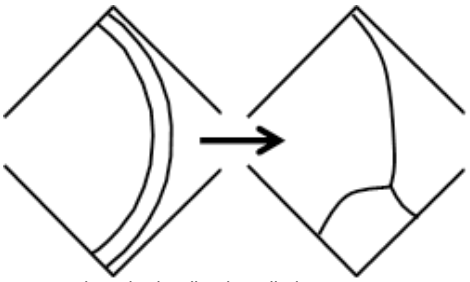

Fig. 4 Schematic of the overlap of lamellae that occurs when the leading lamella jumps to an asymmetric shape. One side of the lamella moves backwards (Figure 2), where it meets the lamella behind it; the bubble between these lamellae is shunted to the pore body, where we assume that it subsequently disappears by diffusion

2.1.1 Diffusion and Convection

We assume that the gas inside the bubbles is an ideal gas, that the overall gas pressure P (used to relate volume to mass in the ideal gas law) is nearly constant in spite of pressure differences between bubbles, and that diffusion across lamellae is characterized by a constant film permeability K. We ignore any effect of Plateau borders on diffusive transport, just as we have neglected any effect on lamella shape above. We represent diffusion rate in terms of the volume of gas transported across the lamella at the pressure and temperature of the foam:

$$\left(\frac{dV}{dt}\right)_{diff} = -\frac{KA(\Delta C_g)}{V_m} = -\frac{KA(\Delta P / R_{ID}T)}{P / R_{ID}T} = -\frac{KA\Delta P}{P} = -\frac{KL^2 P_{ce}}{P} A_D \Delta P_D \tag{4}$$

where V is the gas volume behind the lamella, A lamella area, ΔC_g the difference in molar concentration in the gas phase on the two sides of the lamella, V_m the molar volume of gas, R_{ID} the ideal-gas constant, and T absolute temperature. The sign of dV/dt in Eq. 4 is negative if the difference in pressure across the lamella ΔP is positive (Fig. 3a) because then the rearward bubble loses gas to the forward bubble by diffusion through the lamella.

The maximum rate of diffusion occurs for a lamella just before the jump from Interval 2 to 3, where area is at a maximum. In relating diffusion rate to convection we use the magnitude of the diffusion rate at that point, which we denote with superscript ^{0}, as the characteristic diffusion rate:

$$\left|\frac{dV}{dt}\right|^0_{diff} = \frac{KL^2 P_{ce}}{P} A_D^0 \Delta P_D^0 \quad . \tag{5}$$

We assume a constant injection rate:

$$\left(\frac{dV}{dt}\right)_{conv} = \frac{vV_{tot}}{L} \tag{6}$$

where v is the interstitial velocity of the flowing gas. We define dimensionless time based on the time to traverse one pore in the absence of diffusion:

$$t_D \equiv \frac{v}{L} t \quad . \tag{7}$$

For cases with no convection we define dimensionless time based on diffusion rate (Eq. 4):

$$t_{D,diff} \equiv \frac{KL^2 P_{ce}}{PV_{tot}} A_D^0 \Delta P_D^0 t \quad . \tag{8}$$

We define the ratio of the characteristic diffusion rate of gas to the convection rate as

$$F_{dc} \equiv \frac{\left|\frac{dV}{dt}\right|^0_{diff}}{\left(\frac{dV}{dt}\right)_{conv}} = \frac{KL^2 P_{ce}}{P} A_D^0 \Delta P_D^0 \frac{L}{vV_{tot}} = \frac{KP_{ce}}{vP} A_D^0 \Delta P_D^0 \left(\frac{V_{tot}}{L^3}\right)^{-1} \quad . \tag{9}$$

The last three terms in Eq. 9 depend on pore shape but not pore size. For our pore shape, they are, respectively, A_D^0 =0.8129, ΔP_D^0=0.2603 and $(V_{tot}/L^3)^{-1}$=3.0606. The ratio of diffusive to convective flux increases with film permeability K, as expected, and surface tension (driving the pressure differences between bubbles, reflected in Eq. 9 in the term P_{ce}); for pores of a given geometry, the ratio decreases with increasing size of the pores (decreasing P_{ce}), with increasing pressure (meaning a

given molar flux of gas has less effect on bubble volume) and with increasing superficial velocity v. It is important to note that v here is superficial velocity of the flowing gas fraction, not the superficial velocity of the gas phase averaged over all the trapped gas. Flowing gas saturation can be as little as 1% of total gas saturation (Kil et al. 2011), and v here reflects the velocity of gas that actually flows.

To assess the ratio of characteristic diffusion to convection rates F_{dc} we use the following values. Values for film permeability and surface tension at low pressure are available from Farajzadeh et al. (2011); for CO_2 and N_2 gases at low pressure representative values are 7.85×10^{-2} and 1.31×10^{-3} m/s for film permeability and 0.025 N/m for surface tension. Surface tension can be as low as 0.001 to 0.005 N/m for supercritical CO_2 (Rossen 1996; Chabert et al. 2012). To put bounds on possible values, consider two extreme cases: a CO_2 foam at 5 bar pressure with superficial velocity of flowing gas of 5 m/d (5.79×10^{-5} m/s) and N_2 foam at 40 bar pressure with flowing-gas superficial velocity of 100 m/d (because of small flowing gas fraction). Equation 8 gives $F_{dc} = 8.78$ and 9.1×10^{-4}, respectively, for the two cases. Thus even for flowing foam it is conceivable that the characteristic diffusion rate could be faster than the imposed convection rate, at least at relatively low pressure in the laboratory. The value of F_{dc} for CO_2 foam decreases with increasing pressure. Consider as a third case supercritical CO_2 foam at 335 K and 100 bar with surface tension 0.003 N/m. Assuming diffusion through the film is not too strongly affected by pressure, F_{dc} is about 0.053 instead of 8.78. Thus it is unlikely that in field application of foam the value of F_{dc} for flowing foam is close to 1, though this is possible at low pressure in the laboratory. Of course if convection stops then all lamella movement is from diffusion and $F_{dc} \rightarrow \infty$.

2.1.2 Merging of lamellae

In bulk foams small bubbles disappear as their gas diffuses into larger surrounding bubbles. Cohen et al. (1996) show that, in the absence of convection, small bubbles lodged in pore throats disappear by gas diffusion. Here we find another mechanism of bubble disappearance in porous media: lamellae between sufficiently small bubbles come into contact at the jumps at the pore body, between Intervals 2 and 3 or between Intervals 3 and 4 (Figures 2 and 3b). After this, the small bubble is lodged against the pore wall (Figure 4), where we assume it is bypassed by convection and disappears over time by diffusion. We do not attempt to represent the diffusion process for the bypassed bubble in detail. Instead, in our calculations, when lamellae intersect each other immediately after a jump, the rearward lamella is immediately deleted from the set of lamellae.

In addition, if bubbles are sufficiently close to each other on the pore wall, their Plateau borders can overlap: one of the bubbles would be shunted toward the opposite pore wall and bypassed by subsequent convection. The sort of rearrangement shown in Figure 4 could thus also be triggered by overlapping Plateau borders away from a pore body.

We do not attempt to represent the diffusion process for the bypassed bubble in detail. Instead, we eliminate the rearward lamella immediately when any of the following situations occur:

- When a lamella from Interval 3 intersects a bubble from Intervals 2 or 4. The intersection is indicated by the lamella of the forward bubble contacting one of the pore walls at a point behind that of the forward lamella (Figure 3b).
- When lamellae next to each other have a dimensionless volume difference less than 0.05 (to represent schematically overlapping Plateau borders); in this case we assume that the bubble in between would be shunted off to the wall and disappear shortly afterward.

2.1.3 Trains of Bubbles

To assign initial positions for the lamellae, individual dimensionless bubble volumes are randomly selected from a uniform distribution. For the case of bubbles initially smaller than the pores, the distribution extends from 0 to 1; for bubbles larger than pores, it extends from 1 to 2. The latter case represents bubbles larger than two pores as well; for any bubble volumes greater than one pore, consecutive lamellae do not occupy the same pore and our calculations are therefore identical. In our calculations, we assume 300 bubbles are initially in the train. Lamella position is recorded as the cumulative volume back to the start of the train. Since all pores are identical, pressure difference across the lamella is given by the fractional part of this volume, as shown in Figure 3a. The positions of lamella attachment to the pore walls can also be determined (Figure 3b), and a check made for intersecting lamellae or lamellae close enough to each other that they would merge, as described in the preceding section. In any individual time step, lamellae may move forward or backwards depending on the relative rates of convection and diffusion at that position. Examples in 2D are described in Nonnekes (2012).

For the case in which dimensionless bubble volumes are uniformly distributed between 0 and 1, the initial distribution can include lamellae that immediately violate the conditions above and disappear. About 5% of bubbles have dimensionless volume less than 0.05, and so one lamellae immediately disappears by the second criterion in the previous section. In addition, lamellae in the initially assigned positions can overlap, violating the first condition in the previous section. We find that around 10 to 25 lamellae of our initial 300 disappear immediately when the initial bubble volumes are uniformly distributed between 0 and 1.

3 Results

3.1 No Diffusion - $F_{dc} = 0$

For bubbles larger than pores, without diffusion bubbles simply move forward at a constant volumetric rate. Therefore one expects that the population-average ΔP_D over the period as bubbles move through a single pore is exactly the same as the integral over the corresponding ΔP_D vs. V_D plot in Figure 3a; the train is simply the summation of identical bubbles making identical passages through identical pores (except for the different starting places). One further expects no change in the bubble-size distribution. For a population of 300 bubbles one further expects that the standard deviation of population-average ΔP_D would be $1/\sqrt{300}$ times that for a single lamella, and that 95% of the time the population-average ΔP_D lies within twice this standard deviation of the mean. We find this to be the case (Figure 5).

It is in principle possible, but unlikely, that the average ΔP_D becomes negative for a train of 300 bubbles. According to the Central Limit Theorem, population-average $\Delta P_D = 0$ would lie within one standard deviations of the population mean for a train of about 15, but not 300, bubbles. More important, for trains of 15 bubbles, excursions to twice the average capillary resistance to flow would be fairly common, at which point the given train might be immobilized and other trains mobilized. Once a train is immobilized, lamellae move toward pore throats, as shown in the next section, and capillary resistance to subsequent movement increases.

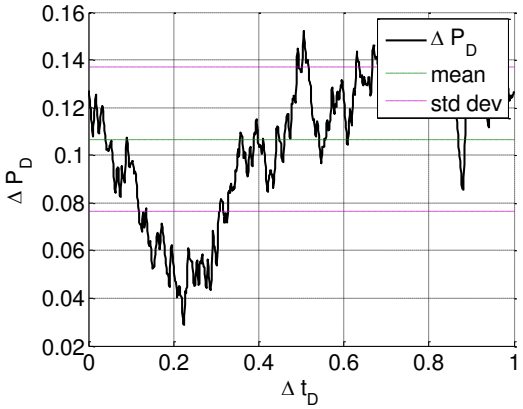

Fig. 5 Progress of a train of bubbles larger than pores with $F_{dc} = 0$: mean $\Delta P_D = 0.1067$; standard deviation = 0.03034. All lamellae traverse one pore in the period shown

Figure 6 shows corresponding results for the case of bubbles initially smaller than pores. In this case 12 lamellae disappear immediately from their initially assigned positions. During movement another 196 lamellae merge during the jumps from Interval 2 to 3 and 3 to 4; thus over two-thirds of the lamellae merge, and the average bubble volume after movement through one pore is greater than the volume of a pore. This occurs because of the large jump in position that a lamella makes going from Interval 2 to 3 and 3 to 4. As noted above, a lamella jumping form Interval 2 to 3 would merge with V_D in the range 0.182 to 0.919. For bubble volumes uniformly distributed between 0 and 1, there is a 74% probability that two adjacent lamellae are close enough to merge at this jump. Thus the jumps play an important role, in addition to diffusion, in eliminating bubbles smaller than pores.

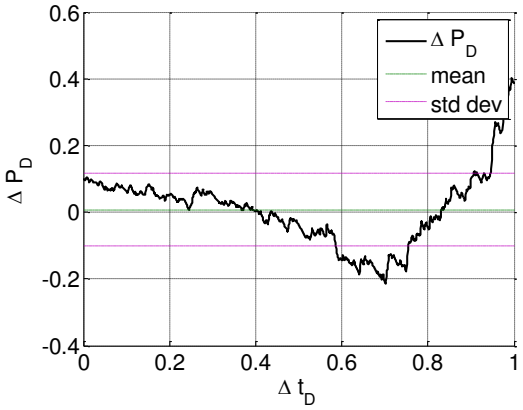

Fig. 6 Progress of a train of bubbles initially smaller than pores with $F_{dc}=0$ (no diffusion): mean $\Delta P_D = 0.00795$; standard deviation=0.1084. Immediately 12 bubbles merge at their initially assigned positions and 196 additional lamellae merge during movement through the first pore

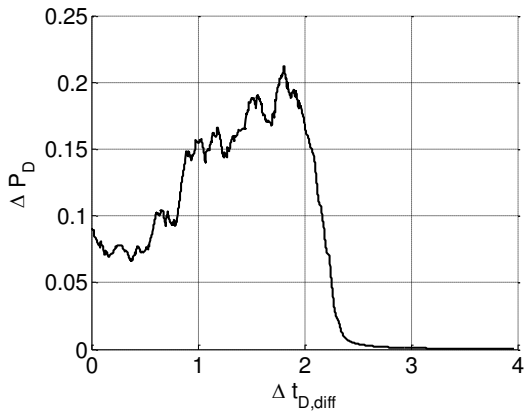

Fig. 7 Evolution of average ΔP_D for a train of bubbles initially smaller than pores, with no imposed convection. 150 bubbles merge; among those 10 merged immediately at their initial positions

The average ΔP_D shown in Figure 6 is an average per lamella; the overall resistance in the train decreases as the number of lamellae decrease. For this case of identical pores, merging occurs only in the transit through the first whole pore; after that the lamellae have and maintain enough space between each other to avoid merging. Beyond this point, movement through each subsequent pore is identical to the movement through the second pore, and in the absence of diffusion no remaining bubbles would merge (see Nonnekes (2012) for examples in 2D). Thereafter the average ΔP_D is exactly as for one lamella, because all remaining lamellae make identical passages through each pore.

3.2 No Convection

The case without convection could reflect a cessation of gas flow on the large scale or immobilization of a bubble train (Falls et al.1988a). In the abandoned path the lamellae then move only by diffusion.

Figure 7 shows the evolution of the average ΔP_D for bubbles initially smaller than pores. Overall, the population-average of ΔP_D initially increases, as lamellae in Interval 2 retreat toward the upstream throat where curvature is great. The trend is opposed by lamellae in Interval 4 approaching the downstream throat, but there are fewer of these. Then ΔP_D decreases as more lamellae move toward the center of the throat, where ΔP_D is zero. For this case, there are 300 bubbles initially but only 150 pore throats, since initial average bubble volume is half the pore volume. As expected, half the lamellae disappear. The diffusion process is essentially complete at a dimensionless time of 2.5. The same dimensionless time suffices for bubbles larger than pores to come to diffusive equilibrium (not shown); in that case bubbles are not the same volume at diffusive equilibrium (some occupy two pores, some occupy one).

Using the cases of the CO_2, supercritical CO_2 and N_2 foams described above, a process lasting $t_{D,diff} = 2.5$ shown in Figure 7 would take about 0.49 s, 8.20 s and 236 s, respectively (cf. Eq. 8). Within a matter of seconds or a few minutes of the end of convection, lamellae would seek out and occupy pore throats.

3.2.1 Convection After a Period of No Convection

Once diffusion has driven all lamellae to pore throats, re-initiating flow requires that they all simultaneously overcome the maximum resistance in the pore throat (Figure 3a), where $\Delta P_D = 1.25$, almost 12 times larger than the average resistance in Figure 3a. It is therefore difficult to remobilize a train once convection has stopped.

3.2.2 Convection and Diffusion

We distinguish three cases, namely convection rate greater than, the same as, or smaller than the nominal diffusion rate ($F_{dc} < 1$, $F_{dc} = 1$, $F_{dc} > 1$). We restrict our attention here to bubbles initially larger than pores.

If convection is greater than the characteristic diffusion rate, the bubbles traverse each pore but spend more time in Intervals 1 and 2 compared to Intervals 3, 4 and 5. Diffusion works against convection in Intervals 1 and 2 but with convection in Intervals 3, 4 and 5. Therefore the population-average ΔP_D is larger than in Figure 5. Figures 8 to 10 present a series of cases with $F_{dc} < 1$, with F_{dc} increasing.

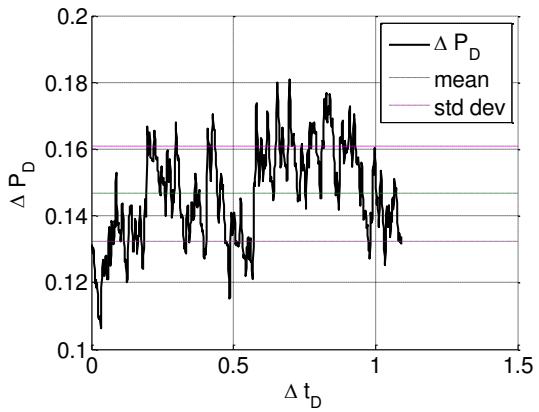

Fig. 8 Convection much greater than diffusion (F_{dc}=0.212): mean ΔP_D=0.1467; standard deviation=0.01432. The train has moved one pore length at t_D = 1.091

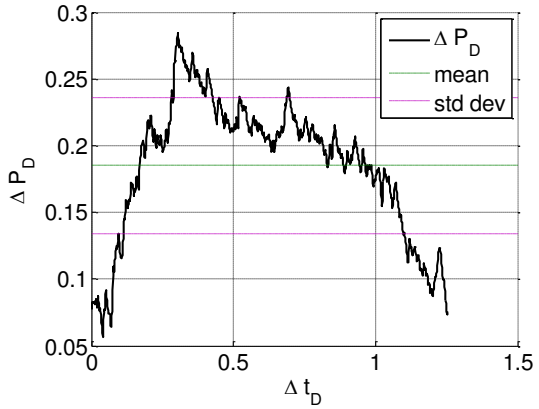

Fig. 9 Convection greater than diffusion (F_{dc}=0.423): mean ΔP_D=0.1851; standard deviation=0.05117. The train has moved one pore length at t_D = 1.253

In Figures 8 to 10, the original positions of the lamellae are randomly assigned, but this distribution is actually not a typical distribution for a case where diffusion is significant. Lamellae traverse Intervals 1 and 2 only slowly but rush through Intervals 3, 4 and 5, since both diffusion and convection act together there. Thus assigning initial lamella positions with equal probability (weighted according to the cumulative volume in each interval, as in Figure 3a) to each interval is an atypical initial distribution. The population-average ΔP_D rises rapidly at first because the lamellae initially in Intervals 3, 4 and 5 are pushed into Intervals 1 and 2, while at the same time the bubbles that began in Intervals 1 and 2 are released at a much slower rate. As the entire population of lamellae has advanced one pore length, it recaptures its original distribution of positions, with much smaller average ΔP_D. However, the time-average ΔP_D over the period during which lamellae advance through one pore is accurate for any initial distribution (as long as bubbles are larger than pores), because in this period all lamellae advance in identical sequences through one pore (though their starting points in the sequence differ). Although it may seem that the value of ΔP_D at the start of the process does not match the value at the end, this is due to the fact that there are over 1000 points displayed in Figures 8 to 10; therefore the first points overlap with the y-axis of the plot and are not clearly visible.

The population-average ΔP_D in Figure 8 is about 37% greater than without diffusion (Figure 5). In this case the volumetric flow rate of gas is unchanged but the pressure difference is increased; thus gas mobility is about 37% less than that of the case with no diffusion. For F_{dc} = 0.423 and 0.635, the increases in ΔP_D are about 73% and 107%. Lamella velocity decreases by 8.3%, 20% and 36% for F_{dc} = 0.212, 0.423 and 0.635 respectively. It is thought that the drag on lamellae scales as roughly the (2/3) or smaller power of lamella velocity (Hirasaki and Lawson 1986; Xu and Rossen 2003). If capillary resistance to flow, quantified here in ΔP_D, accounts for roughly half of the effective viscosity of foam (Falls et al. 1989), then the increase in capillary resistance more than makes up for the reduction in drag on lamellae. Contrary to expectations, then, a large rate of diffusion, by itself, appears to *reduce* gas mobility by increasing the time lamellae spend in positions of large capillary resistance to forward movement. This conclusion depends in part on the relative importance of capillary resistance to flow and drag on moving lamellae.

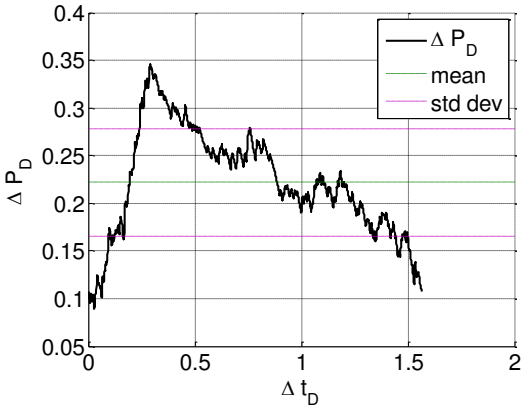

Fig. 10 Convection greater than diffusion (F_{dc}=0.635): mean ΔP_D=0.2218; standard deviation=0.05633. The train has moved one pore length at t_D = 1.564

Our second case is F_{dc} = 1. In this case there is one position, just before the jump from Interval 2, where convection balances diffusion. All lamellae advance until they reach that position. The evolution of population-average ΔP_D is shown in Figure 11; the final value is 2.44 times the value in the absence of diffusion.

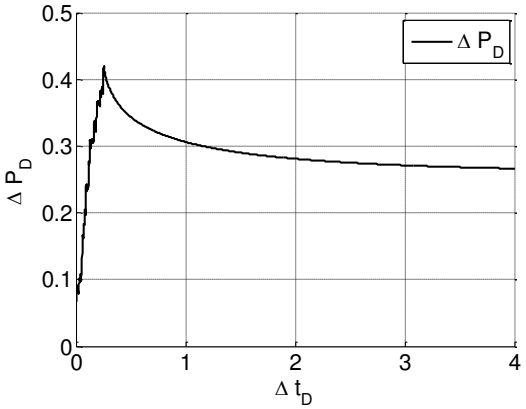

Fig. 11 Convection just balanced with diffusion (F_{dc}=1). Lamellae converge to a single location just before the jump from Interval 2 to Interval 3. Final ΔP_D=0.2603

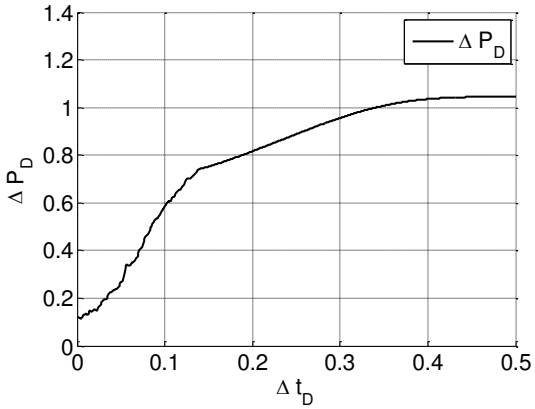

Fig. 12 Diffusion faster than convection: evolution of average ΔP_D for F_{dc}=4; bubbles larger than pores. Lamellae converge to a single location in Interval 2

Our final case is $F_{dc} > 1$: convection smaller than diffusion. In this case there is a position further upstream in Interval 2 where convection balances diffusion. Both convection and diffusion drive lamellae rapidly through Intervals 3, 4 and 5. Lamellae further downstream in Interval 2 retreat until reaching this position. The position where diffusion balances convection can be estimated as follows. Because diffusion just balances convection at this point (cf. Eq. 9)

$$1 = \frac{KP_{ce}}{vP} A_D \Delta P_D \left(\frac{V_{tot}}{L^3} \right)^{-1} \tag{10}$$

and so

$$\frac{1}{F_{dc}} = \frac{A_D}{A_D^0}\frac{\Delta P_D}{\Delta P_D^0}; \quad \Delta P_D = \frac{\Delta P_D^0}{F_{dc}}\frac{A_D^0}{A_D} \quad . \tag{11}$$

ΔP_D increases with increasing F_{dc} for $F_{dc} > 1$, in contrast to the 2D case (Nonnekes et al. 2012). For $F_{dc} > 4.8$ lamellae take a position in Interval 1, and ΔP_D decreases with further increases in F_{dc}. Figure 12 shows the evolution of population-average ΔP_D for $F_{dc} = 4$; other examples in 2D are in Nonnekes (2012). Figure 13 shows the population-average ΔP_D as a function of F_{dc}. The maximum ΔP_D, equal to 1.26, is at $F_{dc} = 4.8$, where the lamella is lodged at the boundary between Intervals 1 and 2.

For $F_{dc} > 1$, all transport of gas is by diffusion; although lamellae do not move, there is still a pressure difference arising from the static curvatures of all lamellae. Indeed, this pressure difference is required to drive the diffusion. Itamura and Udell (1989) propose such a mechanism for gas transport in steam foam (where conduction and evaporation, not diffusion, transport steam through lamellae).

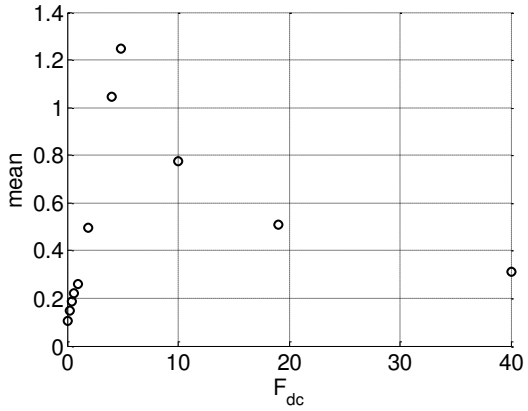

Fig. 13 Population-average ΔP_D as a function of F_{dc}

4 Conclusions and Implications

Our estimates of F_{dc} for field conditions suggest that gas diffusion is a relatively minor contribution to the overall gas flow rate ($F_{dc} << 1$). In that case, unless bubbles are initially smaller than the pores (contradicting current foam models), diffusion does not affect the bubble-size distribution for flowing bubbles, and actually increases the capillary resistance to foam flow modestly. Whether diffusion modestly increases or reduces the overall mobility of foam depends on the relative importance of capillary resistance to flow and the drag on lamellae. Using Eq. 9 one can estimate F_{dc} for other cases. It is possible that F_{dc} is greater than one for fast-diffusing gases at relatively low pressures, in which case it is possible that all gas transport is by diffusion, as conjectured by Itamura and Udell (1989).

Therefore we contend that the greater permeability of CO_2 through foam films is not the cause of markedly greater gas mobility in supercritical CO_2 foams compared to N_2 foams. The results of Falls et al. (1988b) for steam foam probably reflect the instability and rupture of lamellae during rapid condensation and evaporation of steam from the lamella, and not the gradual disappearance of smaller bubbles by mass transfer through lamellae.

If convection stops, our results suggest that diffusion drives lamellae to pore throats in a matter of tens of seconds or minutes under field conditions. Thereafter, re-activating the bubble train along the given path is made much harder by the greater capillary resistance to flow provided by lamellae in pore throats.

In real porous media there are a variety of pore sizes. In the context of our model of a periodically constricted tube, if there is one pore body along the bubble train much wider than others, it is possible that lamellae could balance convection there, immobilizing the lamella, while other lamellae advance on that body and merge with that lamella. This requires not only that lamellae become fixed in some pore bodies, but that they continue to advance through the other pores: the pore-size distribution along the bubble train must therefore be broad. It also requires that F_{dc} for the wide pores be greater than one, but less than one for other pores. Given the small values of F_{dc} that we estimate for typical pore sizes at field pressures, this situation appears unlikely to occur in field applications.

Acknowledgments

We thank Dr. Rouhollah Farajzadeh and Prof. Rumen Krastev for helpful discussions during the preparation of this manuscript.

References

Afsharpoor, A., Lee, G.S. and Kam, S.I.: Mechanistic Simulation of Continuous Gas Injection Period During Surfactant-Alternating-Gas (SAG) Processes Using Foam Catastrophe Theory. Chem. Eng, Sci. **6**, 3615-3631 (2010)

Alvarez, J. M., Rivas, H., Rossen, W.R.: A Unified Model for Steady-State Foam Behavior at High and Low Foam Qualities. SPE J. **6**, 325-333 (2001)

Ashoori, E., Marchesin, D., Rossen, W.R.: Stability Analysis of Uniform Equilibrium Foam states for EOR Processes. Transp. Porous Media **92**, 573-595 (2012)

Bird, R. B., Stewart, W. E., Lightfoot, E. N.: Transp. Phenomena, 2nd Ed., Wiley, New York (2002)

Chabert, M., Morvan, M., Nabzar, L.: Advances Screening Technologies for the Selection of Dense CO2 Foaming Surfactants. Paper presented at the SPE/DOE Symposium on IOR, Tulsa, OK, 14-18 April 2012

Chen, Q., Gerritsen, M.G., Kovscek, A.R.: Modeling Foam Displacement with the Local-Equilibrium Approximation: Theory and Experimental Verification. SPE J. **15**, 171-183 (2010)

Chou, S. I.: Conditions for Generating Foam in Porous Media. Paper presented at the SPE Annual Technical Conference and Exhibition, Dallas, 6-9 Oct 1991

Cohen, D., Patzek, T.W., Radke, C.J.: Two-Dimensional Network Simulation of Diffusion-Driven Coarsening of Foam Inside a Porous Medium. J. Colloid Interface Sci. **179**, 357-373 (1996)

Cox, S.J., Neethling, S., Rossen, W.R., Schleifenbaum, W., Schmidt-Wellenburg, P., Cilliers, J.J.: A Theory of the Effective Yield Stress of Foam in Porous Media: the motion of a soap film traversing a Three-Dimensional Pore. Colloids Surfaces A: Physicochem Eng. Aspects **245**, 143-151 (2004)

Enick, R. M., Olsen, D., Ammer, J., Schuller, W.: Mobility and Conformance Control for CO2 EOR via Thickeners, Foams and Gels - A Literature Review of 40 Years of Research and Pilot Tests. Paper presented at the SPE/DOE Symposium on IOR, Tulsa, OK, 14-18 April 2012

Falls, A.H., Hirasaki, G.J., Patzek, T.W., Gauglitz, P.A., Miller, D.D., Ratulowski, J.: Development of a Mechanistic Foam Simulator: The Population Balance and Generation by Snap-Off. SPERE **3**, 884-892 (1988a)

Falls, A. H., Lawson, J. B., Hirasaki, G. J.: The Role of Noncondensable Gas in Steam Foams. J. Petr. Technol. **40**, 95-104 (1988b)

Falls, A.H., Musters, J. J., Ratulowski, J.: The Apparent Viscosity of Foams in Homogeneous Bead Packs. SPE J. **4**, 155-164 (1989)

Farajzadeh, R., Andiranov, A., Bruining, J., Zitha, P. L. J.: Comparative Study of CO_2 and N_2 Foams in Porous Media at Low and High Pressure-Temperatures. Ind. Eng. Chem. Res. **48**, 4542-4552 (2009)

Farajzadeh, R., Muruganathan, R. M., Krastev, R., Rossen, W. R.: Effect of Gas Type on Foam Film Permeability and Its Implications for Foam Flow in Porous Media. Adv. Colloid Interface Sci. **168**, 71–78 (2011)

Hatziavrimidis, D.: Stability of thin evaporating/condensing films in the presence of surfactants. Intl. J. Multiphase Flow **18**, 517–530 (1992)

Hirasaki, G. J.: The Steam-Foam Process. J. Petrol. Technol. **41**, 449-456 (1989)

Hirasaki, G. J., Lawson, J. B.: Mechanisms of Foam Flow through Porous Media - Apparent Viscosity in Smooth Capillaries. SPE J. **25**, 176-190 (1985)

Itamura, M. T., Udell, K. S.: The Role of Noncondensible Gases in Heat and Mass Transfer in Porous Media Containing a Steam Foam. Multiphase Flow, Heat and Mass Transfer, ASME HTD **109**, 87-92 (1989)

Kibodeaux, K. R.: Experimental and Theoretical Studies of Foam Mechanisms in Enhanced Oil Recovery and Matrix Acidization Applications. PhD dissertation, The University of Texas at Austin, (1997)

Kil, R. A., Nguyen, Q. P., Rossen, W. R.: Determining Trapped Gas in Foam From CT Images. SPE J. **16**, 24-34 (2011)

Kralshevsky, P. A. Danov, K. D., Ivanov, I. B.: Thin Liquid Film Physics. in R. K. Prud'homme and S. Khan, ed., Foams: Theory, Measurements and Applications, Marcel Dekker, New York, pp. 2-89 (1996)

Kuhlman, M. I.., Falls. A. H., Hara, S. K., Monger, T. G., Borchardt, J. K.: Carbone Dioxide Foam with Surfactants Used Below Their Critical Micelle Concentration. SPERE **5**, 445-452 (1990)

Marsden, S. S.: Foams in Porous Media. US DOE rep. DOE/SF/11564-15 (DE8600290), (1986)

Nonnekes, L. E.: Effect of Diffusion on Foam Bubble Size Distribution and Gas Mobility: an Idealized 2D Model. BSc thesis, Delft U. of Technol., (2012)

Nonnekes, L. E., Cox, S. J., Rossen, W. R.: A 2D Model for the Effect of Gas Diffusion on Mobility of Foam for EOR. Paper presented at the 12th European Conference on the Mathematics of Oil Recovery, Biarritz, France, 10-13 Sept. (2012)

Rossen, W.R.: Theories of Foam Mobilization Pressure Gradient. Paper presented at the SPE/DOE Enhanced Oil Recovery Symposium, Tulsa, OK, 17-20 April (1988)

Rossen, W.R.: Theory of Mobilization Pressure Gradient of Flowing Foams in Porous Media. I. Incompressible Foam. J. Colloid Interface Sci. **136**, 1-16 (1990a)

Rossen, W.R.: Theory of Mobilization Pressure Gradient of Flowing Foams in Porous Media. II. Effect of Compressibility. J. Colloid Interface Sci. **136**, 17-37 (1990b)

Rossen, W.R.: Theory of Mobilization Pressure Gradient of Flowing Foams in Porous Media. III Asymmetric Lamella Shapes. J. Colloid Interface Sci. **136**, 38-53 (1990c)

Rossen, W.R.: Minimum Pressure Gradient for Foam Flow in Porous Media: Effect of Interactions with Stationary Lamellae. J. Colloid Interface Sci. **139**, 457-468 (1990d)

Rossen, W.R..: Foams in Enhanced Oil Recovery. in R. K. Prud'homme and S. Khan, ed., Foams: Theory, Measurements and Applications, Marcel Dekker, New York, pp. 413-464 (1996)

Weaire, D., Hutzler, S.: The Physics of Foams. Clarendon Press, Oxford, (1999)

Xu, Q., Rossen, W. R.: Effective Viscosity of Foam in Periodically Constricted Tubes. Colloids Surfaces A: Physicochem Eng. Aspects **216** (1-3), 175-194 (2003)